MODELLING PERMANENT INDENTATION IN COMPOSITE SUBJECTED TO IMPACT: IDENTIFICATION THROUGH A SPECIFIC THREE-POINT BENDING TEST

N. Hongkarnjanakul[a], S. Rivallant[a*], C. Bouvet[a]

[a]*Université de Toulouse ; INSA, UPS, Mines Albi, ISAE ; ICA (Institut Clément Ader), 10 avenue Edouard Belin – 31055 Toulouse - France*
**samuel.rivallant@isae.fr*

Keywords: Permanent indentation, Impact behaviour, Damage tolerance, Three-point bending test

Abstract
This paper presents a study on the mechanisms leading to permanent indentation in composite laminates subjected to low-velocity impact. A three-point bending test on laminated beams is used. During loading, matrix cracks appear. When unloading, it is shown that cracks cannot close entirely, due to debris inside matrix cracks and the formation of cusps where mixed-mode delamination occurs. The addition of all these non-closure in a laminate is assumed to be the origin of permanent indentation under impact loading. Then, a simple physically-based law of permanent indentation is proposed. This law is qualitatively tested with a three-point bending FE model and applied in a low-velocity impact FE model to predict permanent indentation. A comparison between experiments and models is presented.

1. Introduction

In recent years, the use of composite structures has increased in aeronautics. Unfortunately, composite materials are often brittle, and impacts like tool drops during manufacturing or maintenance can lead to damage inside the material, with a severe reduction of strength of the structure, but with a very little mark left onto the surface. Therefore the concept of Damage Tolerance was defined for impact on composite: a composite structure must be designed so that it can sustain the ultimate load even when damaged. One of the key points in such a concept is the detection of damage. In practice, damage is detected from the permanent indentation (dent depth) due to the impact, and the "Barely Visible Impact Damage" (BVID) is defined as the threshold level at which the damage is detectable. Understanding of permanent indentation mechanism is therefore essential to allow for designing composite structures with respect to damage tolerance.
In the last decades, a number of researchers have studied damage due to low-velocity impact [1-5]. However, the phenomenon of permanent indentation is still not very well understood [2,3,6-9]. In the literature, different kinds of model can be found to predict permanent indentation. Some are analytical predictions based on the fitting of numerous experimental data of low-velocity impact tests on composite laminates [7,8]. Others are based on FE analysis, with continuum damage mechanics [3-5,9], taking into account the nonlinear shear behaviour (more often the plasticity) in the ply or in the interface. Abi Abdallah et al. [6]

claim that the permanent indentation is due to the debris getting stuck inside matrix cracks and blocking the closure of cracks.
The aim of this paper is to study the mechanisms involved in permanent indentation in order to propose a model for FE simulation of impact and to propose a way to identify its parameters independently. Thus, a three-point bending test is chosen for this study. It enables the creation of matrix cracks and the observation of their evolution: opening, closure and eventual blocking of closure. The mechanism of crack opening/closure, especially in the out-of-plane direction, is highlighted. A simple law of permanent indentation is then presented, with a single parameter identified from the experiments. Finally, indentation law is applied in a FE impact model and a comparison with experimental results is done.

2. Experimental study

2.1. Material and test setup

Three-point bending tests are conducted with a 0.3 mm/min displacement rate. Specimens are 50×10 mm^2 (length×width) laminates made of T700/M21 CFRP. Two stacking sequence configurations are used: $[0,90_6,0]$ (specimen I1, 2 mm thick) and $[0_2,90_2,0_2]$ (specimens I2-A, I2-B and I2-C : 1.5 mm thick). To generate matrix cracking in the 90° plies - due to shear - without tensile or compressive fibre failure in the external 0° plies, the span (distance between lower supports) is chosen equal to 10 mm. The three cylinder supports are 6 mm in diameter. During the tests, a digital camera is used.
With such a short span, local deformation (δ^{local}) due to high contact pressure between the specimen and the cylinder supports (fig.1a) can be significant compared to shear and bending effects [10]. Thus the global displacement obtained from the machine (δ^{global}) must be corrected to obtain the bending displacement ($\delta^{bending}$), that we want to measure (fig.1b). δ^{local} is evaluated thanks to 2D DIC in the composite, whereas δ^{global} is calculated from the movement of the cylinders (also with DIC, applied to the cylinders). Hereafter in this paper, unless otherwise specified, the term "displacement" is used for "bending displacement".

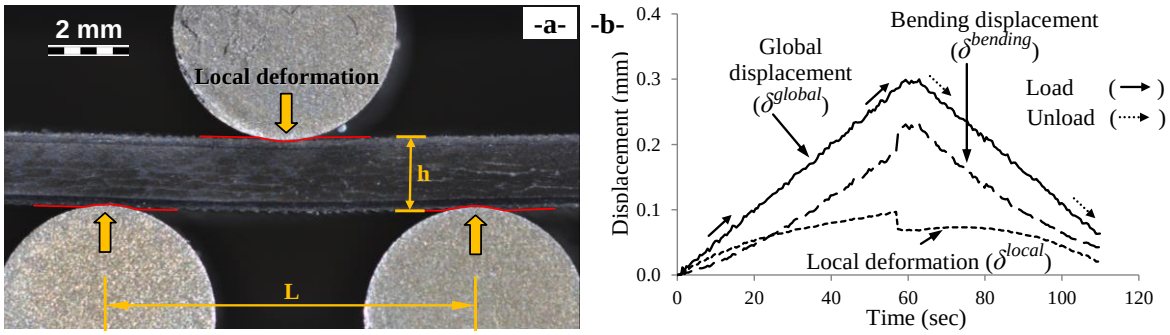

Figure 1. (a) Three point bending test on specimen I1 - (b) Displacement/Time curves for specimen I1

2.2. Opening and closure of matrix cracks

The three-point bending test is carried out with only one cycle of loading and unloading. Many tests were performed, but only four specimens with only a single crack and no fibre rupture were analysed, so that only the influence of matrix cracks could be studied. The results from specimen I1 are presented in fig.2. The specimen is loaded until a 45° matrix crack appears in the 90° ply (with delamination also) which can be noticed due to the load drop at state 2-3: when the matrix crack occurs, the specimen's rigidity suddenly decreases but the global displacement (imposed) remains the same. As a consequence, the force

decreases, the local deformation is released and the bending displacement increases (see also fig.1b). The out-of-plane crack width δ_z is also measured by using DIC. Unloading is then applied and the crack width gets smaller (state 3-4-5). At the end of the test (point 5), one can notice that there is a residual crack opening when the force is null. This phenomenon is assumed to be the origin of the formation of permanent indentation.

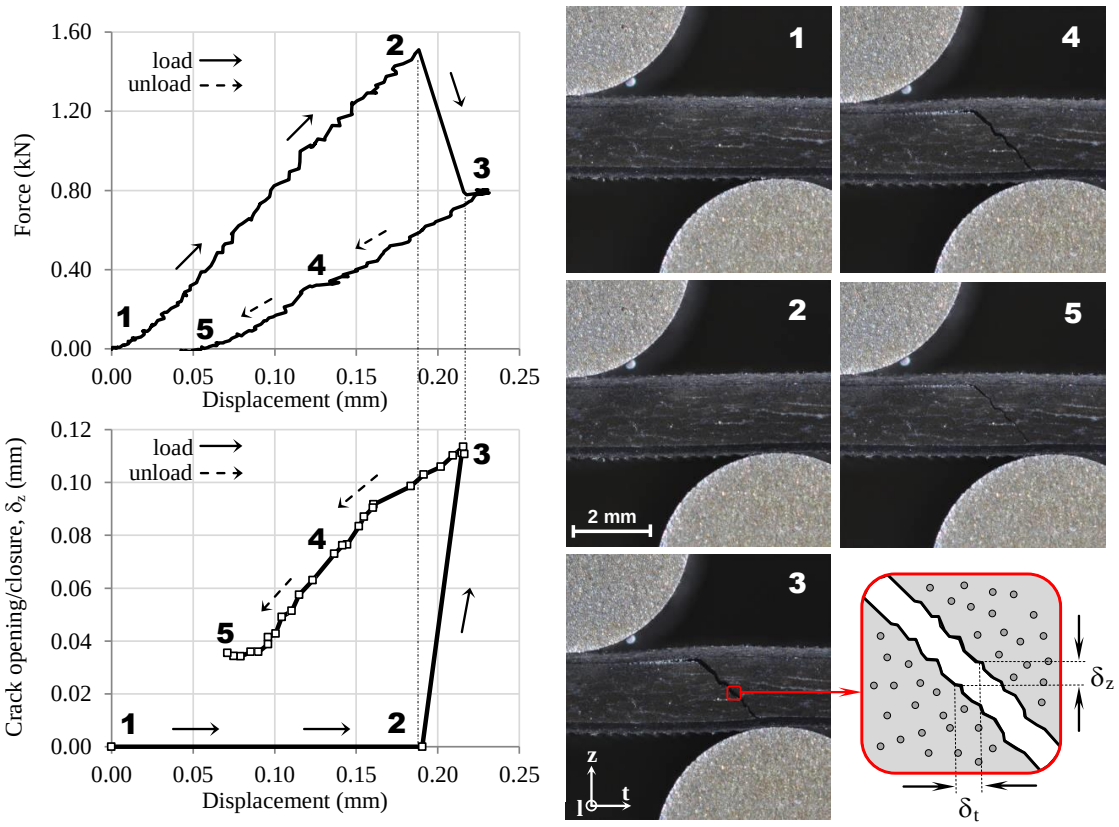

Figure 2. Observation of the evolution of crack opening/closure on the right part of specimen I1

Three additional tests on configuration I2 are also performed but different load cases are introduced. The load is continuously applied after the onset of crack initiation to three different levels of additional displacements, i.e. 0.02 mm, 0.08 mm, and 0.15 mm for specimens I2-A, I2-B, and I2-C, respectively (fig.3a). The results exhibit some scatters in the onset of crack formation data for these tests, but different crack widths are obtained according to the different additional displacements (fig.3b).

Evolution of crack opening/closure δ_t and δ_z is determined at the centre of the matrix cracks, where the subscripts *t* and *z* denote transverse and out-of-plane directions respectively (fig.2). The results of non-dimensional crack evolution, i.e. δ_t/δ_t^{max} and δ_z/δ_t^{max}, reveal a convergence for all tests. That is, using non-dimensional values of displacement and crack opening/closure, the shape of crack closure/displacement curves for all tests are similar, and regardless of how big the maximum crack opening is, the final crack width after unloading is around 20% - 40% of maximum crack opening (fig.3c) for both crack directions (t and z) and for both specimen configurations.

In order to investigate the cause of this non-zero width, a microscopic observation is performed (fig.4: optical microscope for full thickness pictures – SEM for cracks details). The micrographs show the 45° crack, and the delamination for specimens I1 and I2-B. Debris are clearly visible inside the cracks. Detailed micrographs show another mechanism leading to the non-closure of cracks: the classical formation of cusps in the ply interface, due to a mixed mode delamination.

According to these observations, we found that the main mechanisms leading to permanent indentation are both the accumulation of debris inside matrix cracks, and the presence of cusps (entirely or partially formed) inside delamination interfaces. Moreover, measurements of the opening/closure of cracks show that the final crack width depends on the maximum width reached during opening of the crack in the test, around 30%.

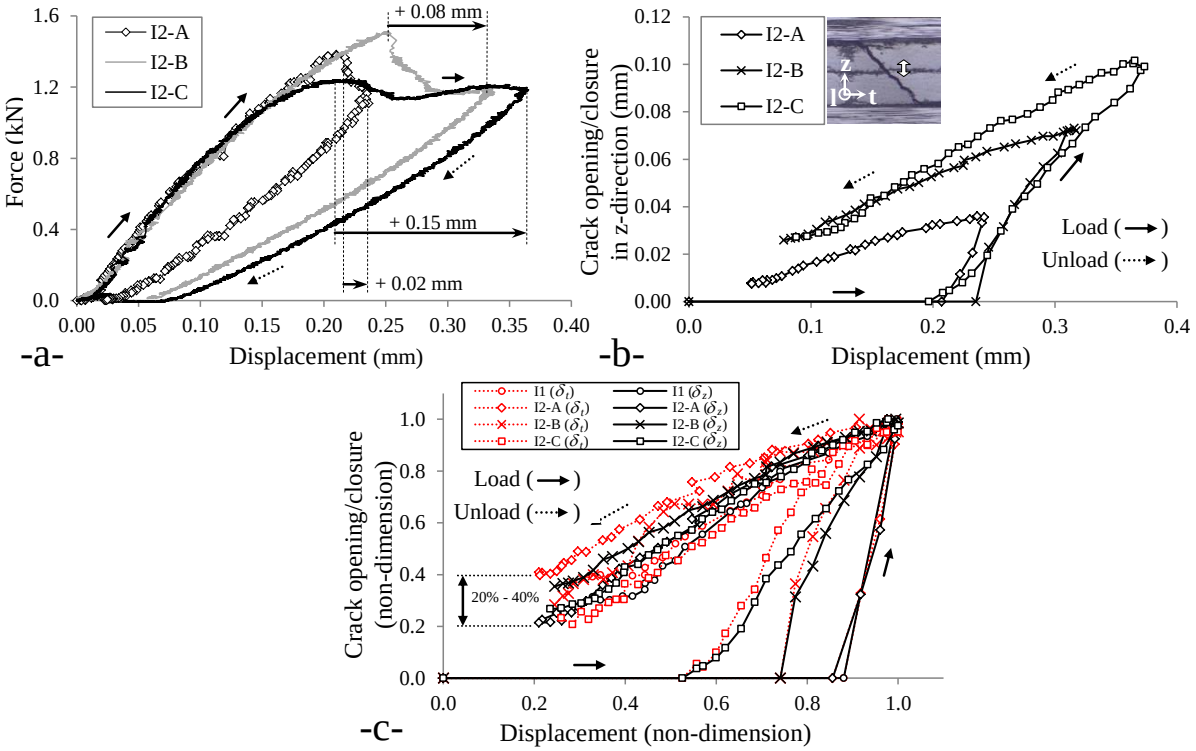

Figure 3. (a) Force-displacement curves for specimens I2-A, B and C - (b) Crack opening/closure for specimens I2-A, B and C - (c) Non-dimensional crack opening/closure for specimens I1, I2-A, B and C

3. Modelling of permanent indentation and application to low-velocity impact

3.1. Permanent indentation law

Results from experiments show that, from a meso-scale point of view, the final matrix crack width is proportional to the maximum crack width reached during the test. It leads to the definition of the crack closure coefficient μ, expressed as $\delta^0 = \mu.\ \delta^{max}$, where δ^0 is the final crack width, after unloading, and δ^{max} is the maximum crack width ever reached during the crack opening. This relation is the fundamental relation that drives the formation of permanent indentation, called "pseudo-plasticity" model. This law includes both the blocking of debris and resin plasticity in plies and interfaces. It can be written for each crack opening direction: transverse and out-of-plane (eq.1):

$$\delta_t^0 = \mu_t \cdot \delta_t^{\max} \ \ if \ \ \delta_t \geq 0 \quad , \text{ and } \quad \delta_z^0 = \begin{cases} \mu_z \cdot \delta_z^{\max} \ \ if \ \ \delta_z \geq 0 \\ \mu_z \cdot \delta_z^{\min} \ \ if \ \ \delta_z < 0 \end{cases} \qquad (1)$$

Where δ_t^0 , δ_z^0 are the final crack-closure width in transversal and out-of-plane directions, respectively. Furthermore, the crack closure coefficient for both directions is assumed to be identical (μ_t=μ_z) due to the fact that the matrix cracks are at an angle close to 45°, which is confirmed by the results shown in fig.3c.

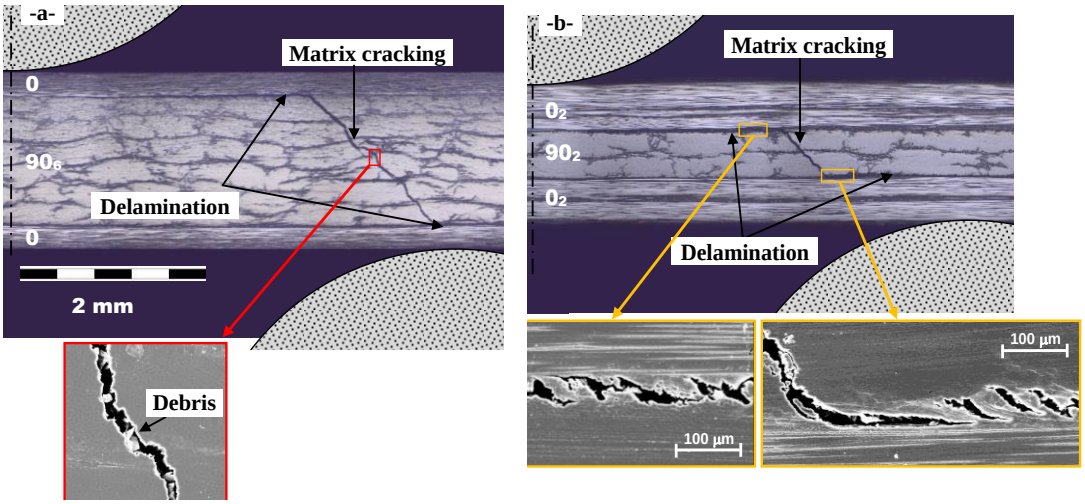

Figure 4. Post mortem observation: specimen I1 (a) and I2-B (b)

3.2. Validation of permanent indentation law on three-point bending test

The objective of this section is to qualitatively test the proposed indentation law with a three-point bending FE model, and understand the interaction of crack opening/closure on the particular discrete ply model (DPM). Mesh types and material laws/properties are based on the impact model from [1,2] in which three damage types are considered namely fibre failure, matrix cracking, and delamination, as shown in fig.5. Dynamic explicit analysis is also maintained with a reasonably slow velocity (0.1 mm/s) to eliminate dynamic problem.
The experimental investigation in the previous section showed that crack non-closure is due to both matrix cracking and delamination; but at meso-scale, it can be considered as a non-closure law only applied in the matrix cracks. The permanent indentation law is integrated inside vertical interface elements where matrix cracking is assigned. To identify the damage that occurred from experiment test, only one row of interface elements is allowed to have matrix cracking with the purpose to simulate the 45° matrix cracking. Thus, the element size is chosen according to the location of 45° matrix cracking, and to respect cohesive zone model for delamination. Fig.6 shows the mechanism of crack opening/closure that corresponds with the permanent indentation law in vertical interface elements.

Initiation of matrix cracking
Before reaching the onset of matrix cracking, the behaviour of vertical interface is elastic: the interface elements connect their neighbouring volume elements by the interface stiffness K (assumed to be very high: 500 000 MPa/mm), defined in three directions (eq.2):

$$\sigma_t = K \cdot \delta_t \quad , \quad \tau_{lt} = K \cdot \delta_l \quad , \quad \tau_{zt} = K \cdot \delta_z \tag{2}$$

Initiation of crack is ruled by matrix tensile failure (eq.3) based upon Hashin's criterion. This criterion is assigned into neighbouring volume elements, but responded in interface elements.

$$\left(\frac{\left\langle \sigma_t^V \right\rangle^+}{\sigma_t^f} \right)^2 + \frac{\left(\tau_{lt}^V\right)^2 + \left(\tau_{tz}^V\right)^2}{\left(\tau^f\right)^2} \leq 1 \tag{3}$$

Where σ_t^V, τ_{lt}^V, τ_{tz}^V are the stresses calculated in neighbour volume elements, σ_t^f is the transverse tensile failure stress, and τ^f is the in-plane shear failure stress. The mechanical characteristics of T700/M21 are given in table1.

The purpose of this three-point bending model is to validate the crack opening/closure simulation. The failure stresses are modified to overcome the possible dispersion of rupture value in experimental tests, so that the cracks can appear at the same time for both experiment and simulation. For example, the values of σ_t^f and τ^f, equal to 60 MPa and 110 MPa respectively, are replaced by 39 MPa and 78 MPa for modelling case I2-B.

	Density	1600 kg/m^3		Ply thickness	0.25 mm
E_l^{tens}	Tensile Young's modulus (fibre direction)	130 GPa	σ_t^f	Tensile failure stress in transverse direction	60 MPa
E_l^{comp}	Compression Young's modulus (fibre direction)	100 GPa	τ^f	In-plane shear failure stress	110 MPa
E_t	Transverse Young's modulus	7.7 GPa	K	Interface element stiffness of matrix cracking	500000 MPa/mm
G_{lt}	Shear modulus	4.8 GPa			
ν_{lt}	Poisson's ratio	0.33	μ	Crack closure coefficient	0.3

Table 1. Mechanical characteristics of T700/M21 unidirectional ply

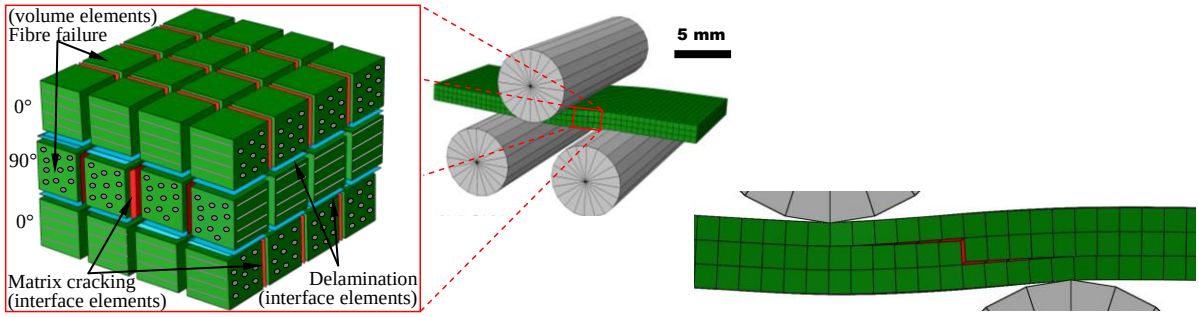

Figure 5. Three-point bending model and elements types

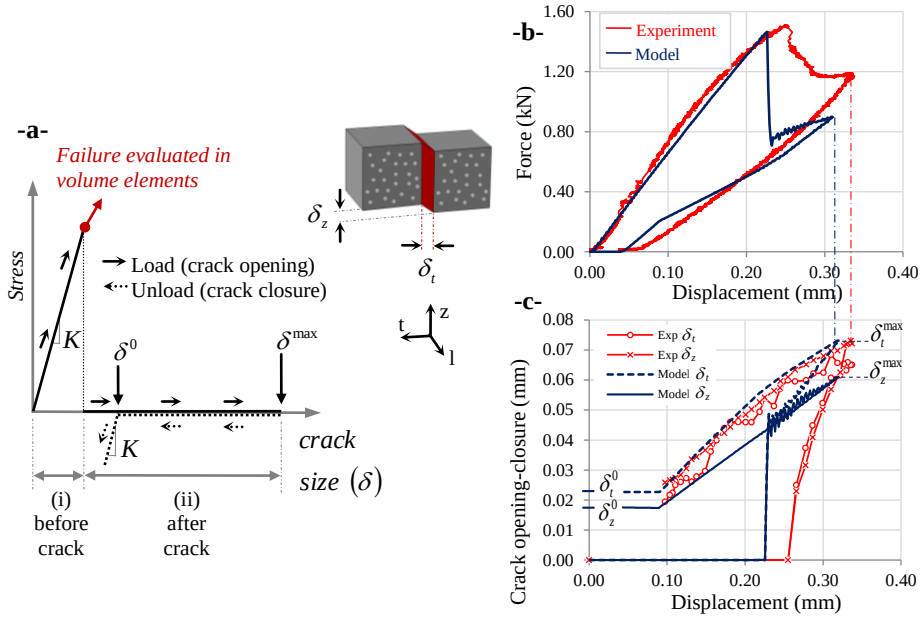

Figure 6. Permanent indentation law representing matrix cracking interface elements (a) Experimental validation of (b) force-displacement response and (c) crack opening/closure for case study I2-B

Opening and closure of cracks

Once the matrix cracking criterion in volume elements (eq.3) is reached (initiation of crack), the adjacent interface elements lose their rigidity, their stresses in all directions turn to zero, and the crack instantaneously opens. The delamination, ruled with a conventional criterion from fracture mechanics in the horizontal interface elements, can also appear.

When the crack tends to close, during unloading, the crack closure law (fig.6a) is applied only in the interface elements for matrix cracking. As long as the crack width is larger than the

final crack closure widths, δ_t^0 and δ_z^0 expressed previously, the crack freely closes with no force in the interface. But if the crack closure goes below these thresholds, a rigidity is applied to prevent closure in the z and t directions. The crack closure law is given in eq.4.

$$\sigma_t = \begin{cases} 0 \ if \ \ \delta_t > \delta_t^0 \\ K \cdot \left(\delta_t - \delta_t^0\right) \ if \ \ \delta_t \le \delta_t^0 \end{cases} \ , \ \tau_{lt} = 0 \ , \ \tau_{zt} = \begin{cases} 0 \ if \ \ \left|\delta_z\right| > \left|\delta_z^0\right| \\ K \cdot \left(\delta_z - \delta_z^0\right) \ if \ \ \left|\delta_z\right| \le \left|\delta_z^0\right| \end{cases} \qquad (4)$$

Experiment tests show that the final crack width is about 20% to 40% of the maximum crack opening. Therefore, an average value of 30% is taken as average crack closure coefficient, that is, μ_t=μ_z=0.3.

The validation of the model of three-point bending is done for all four test cases and gives similar agreement; but only results of the case I2-B are presented here (fig.6). Both force/displacement and crack closure/displacement curves show a good agreement with tests, even if the load release after crack initiation is overestimated.

Impact on plates

The indentation law presented above is then implemented in an existing model of low-velocity impact on T700/M21 laminated plates to improve the prediction of permanent indentation given by the previous indentation law [1]. The description of the model (except indentation law) can be found in [1], the lay-ups (C_1, C_2, D_1, D_2, E_1, E_2) and tests configurations in [2]. Two values of parameters μ are tested: μ_t=μ_z=0.3 and 0.35.

In most of the case, 0.35 give the best results (fig.7). The maximum difference in permanent indentation between experiment and simulation is 24%, and the tendency is well reproduced. More information is available in [11].

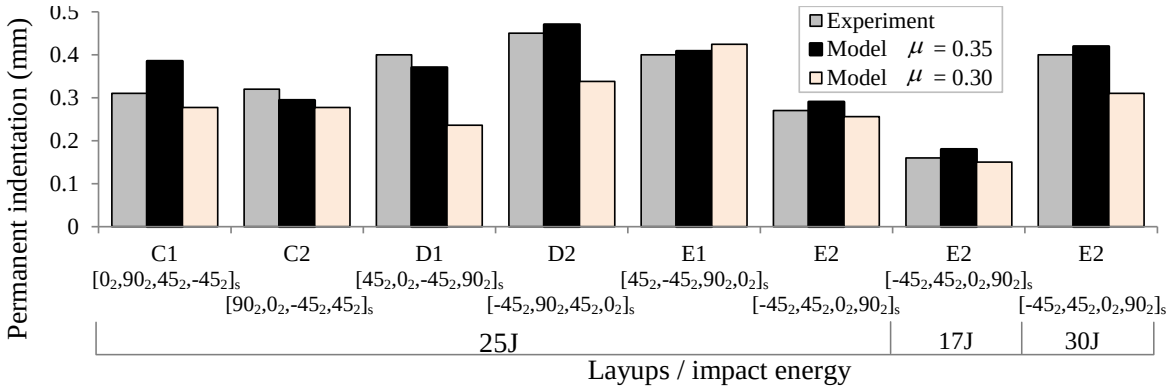

Figure 7. Comparison of permanent indentation on eight test cases, varying layups and impact energies

4. Conclusion

In the present paper a model of permanent indentation due to low-velocity impact is proposed using a three-point bending test. An experimental observation of matrix crack opening/closure leads to the explanation of the origin of permanent indentation. When a matrix crack appears, it does not completely close and remains at approximately 30% of maximum crack opening, observed in both transversal and out-of-plane directions. This unclosed crack is due to the blocking of debris inside matrix cracking, and cusp formation due to mixed mode in delamination. Thanks to these observations, a material law for indentation is proposed, based on the crack closure coefficient.

This “pseudo-plastic” law is initially tested with three-point bending model based upon a selected case study (I2-B) with the aim of understanding how the crack opening/closure

mechanism interacts with the discrete model. Consequently, the same law is validated on low-velocity impact model, and the crack closure coefficient is found to directly affect the value of permanent indentation.
The advantages of the proposed law are its simplicity, and the need for only one single parameter which can be found from a three-point bending test, or numerically adjusted.
The possibility to predict the permanent indentation due to a low velocity impact with a numerical simulation enables to find the energy to reach BVID, and then to launch a complete calculation taking into account impact, permanent indentation and Compression After Impact, in order to predict the residual strength of a composite laminate with respect to Damage Tolerance concept, as in [12].

Acknowledgments

This work was granted access to the HPC resources of CALMIP.
The authors also gratefully acknowledge the partial financial support through the THEOS Operation Training Program (TOTP).

References

[1] Bouvet C, Rivallant S, Barrau J-J. Low velocity impact modeling in composite laminates capturing permanent indentation. *Compos Sci Technol* 2012;72(16):1977-1988
[2] Hongkarnjanakul N, Bouvet C, Rivallant S. Validation of low velocity impact modelling on different stacking sequences of CFRP laminates and influence of fibre failure. *Compos Struct* 2013;106:549-559
[3] Donadon MV, Iannucci L, Falzon BG, Hodgkinson JM, de Almeida, SFM. A progressive failure model for composite laminates subjected to low velocity impact damage. *Compos Struct* 2008;86(11-12):1232-1252
[4] Faggiani A, Falzon BG. Predicting low-velocity impact damage on a stiffened composite panel. *Compos Part A:* 2010;41(6):737-749
[5] Shi Y, Swait T, Soutis C. Modelling damage evolution in composite laminates subjected to low velocity impact. *Compos Struct* 2012;94(9):2902-2913
[6] Abi Abdallah E, Bouvet C, Rivallant S, Broll B, Barrau J-J. Experimental analysis of damage creation and permanent indentation on highly oriented plates. *Compos Sci Technol* 2009;69(7-8):1238-1245
[7] Caprino G, Lopresto V. The significance of indentation in the inspection of carbon fibre-reinforced plastic panels damaged by low-velocity impact. *Compos Sci Technol* 2000;60(7):1003-1012
[8] Caprino G, Langella A, Lopresto V. Indentation and penetration of carbon fibre reinforced plastic laminates. *Compos Part B* 2003;34(4):319-325
[9] He W, Guan Z, Li X, Liu D. Prediction of permanent indentation due to impact on laminated composites based on an elasto-plastic model incorporating fiber failure. *Compos Struct* 2013;96:232-242
[10] Mujika F. On the effect of shear and local deformation in three-point bending tests. *Polym Test* 2007;26(7):869-877
[11] Hongkarnjanakul N, Rivallant S, Bouvet C, Miranda A. Permanent indentation characterization for low-velocity impact modelling using three-point bending test. J *Compos Mater* Online August 2013
[12] Rivallant S, Bouvet C, Hongkarnjanakul N. Failure analysis of CFRP laminates subjected to Compression After Impact: FE simulation using discrete interface elements. *Compos Part A* 2013;55:83-93